



THE UNIVERSITY *of* EDINBURGH

Edinburgh Research Explorer

Oil sands in glacial till as a driver of fast flow and instability in the former Laurentide Ice Sheet: Alberta, Canada

Citation for published version:

McCerery, R, Woodward, J, Winter, K, Esegbue, O, Jones, M & McHale, G 2023, 'Oil sands in glacial till as a driver of fast flow and instability in the former Laurentide Ice Sheet: Alberta, Canada', *Earth Surface Processes and Landforms*. <https://doi.org/10.1002/esp.5700>

Digital Object Identifier (DOI):

[10.1002/esp.5700](https://doi.org/10.1002/esp.5700)

Link:

[Link to publication record in Edinburgh Research Explorer](#)

Document Version:

Publisher's PDF, also known as Version of record

Published In:

Earth Surface Processes and Landforms

General rights


Copyright for the publications made accessible via the Edinburgh Research Explorer is retained by the author(s) and / or other copyright owners and it is a condition of accessing these publications that users recognise and abide by the legal requirements associated with these rights.

Take down policy

The University of Edinburgh has made every reasonable effort to ensure that Edinburgh Research Explorer content complies with UK legislation. If you believe that the public display of this file breaches copyright please contact openaccess@ed.ac.uk providing details, and we will remove access to the work immediately and investigate your claim.



Oil sands in glacial till as a driver of fast flow and instability in the former Laurentide Ice Sheet: Alberta, Canada

Rebecca McCerery¹  | John Woodward¹ | Kate Winter¹ | Onoriode Esegbue² | Martin Jones² | Glen McHale³

¹Department of Geography and Environmental Sciences, Faculty of Engineering and Environment, Northumbria University, Newcastle-upon-Tyne, UK

²School of Natural and Environmental Sciences, Faculty of Science, Agriculture and Engineering, Newcastle University, Newcastle-upon-Tyne, UK

³Institute for Multiscale Thermofluids, School of Engineering, University of Edinburgh, Edinburgh, UK

Correspondence

Rebecca McCerery, Department of Geography and Environmental Sciences, Faculty of Engineering and Environment, Northumbria University, Newcastle-upon-Tyne, NE1 8ST, UK.

Email: r.mccerery@northumbria.ac.uk

Funding information

Northumbria University Research Development Fund

Abstract

Reconstructions of the southwestern Laurentide Ice Sheet (LIS) from geomorphology have revealed complex cross-cutting ice streams, indicative of surging and flow switching. This flow pattern and behaviour is distinct from the rest of the ice sheet where ice streams flowed radially to the ice sheet margin. Many ice streams in the southwestern sector originate around the Alberta Oil Sands (AOS). Previous reports have detected oil sands material in surficial and glacial sediments south of the AOS, demonstrating potential glacial mobilisation of the oil sands. In this study, we use geochemical fingerprinting to systematically investigate surficial sediments from the former Central Alberta Ice Stream (CAIS) flow track. We compare the geochemical signatures of 82 sediments from within and outside the CAIS limits with those of the AOS (from mines and natural exposures), using gas chromatography–mass spectrometry oil–oil correlation techniques. Our results provide geochemical evidence of glacial erosion and long-distance mobilisation of AOS producing contamination signatures in sediments throughout the CAIS flow track. The strength of the AOS signature is particularly strong in sediments along the terminating margins, to the east of Calgary and in the Cooking Lake area to the southeast of Edmonton. These results inform theoretical models of enhanced slipperiness, inspired by slippery liquid infused porous surfaces (SLIPS), whereby oil lubrication of the basal sediment influences the degree of sliding and basal deformation in the ice stream. We hypothesise that naturally occurring hydrocarbons at the basal interface exerted control on the location of the onset zone of the CAIS and surrounding ice streams in Alberta. The enhanced slipperiness caused by oil contamination may also explain ice streaming and surging in other ice sheets, such as the Barents Sea Ice Sheet, where hydrocarbons are known to have been driven to the sedimentary interface during glaciation.

KEYWORDS

basal sliding, biomarkers, glacial erosion, glaciation, organic geochemistry, petroleum hydrocarbons, quaternary, SLIPS, subglacial deformation

1 | INTRODUCTION

The extent, retreat and also flow pattern of the Laurentide Ice Sheet (LIS) is well understood, and it is one of the most widely reconstructed

palaeo ice sheets (Stokes & Clark, 2001; Winsborrow, Clark, & Stokes, 2004). These reconstructions from geomorphology and sedimentology show complex and cross-cutting ice streaming in the southwestern Interior Plains of the Alberta and Saskatchewan with, at times, evidence of overprinting and ice streams running parallel to the ice sheet boundary (Figure 1) (Margold, Stokes, & Clark, 2015). The

Funding This research was funded by Northumbria University Research Development Fund.

This is an open access article under the terms of the [Creative Commons Attribution](https://creativecommons.org/licenses/by/4.0/) License, which permits use, distribution and reproduction in any medium, provided the original work is properly cited.

© 2023 The Authors. *Earth Surface Processes and Landforms* published by John Wiley & Sons Ltd.

landform assemblages in the region are reflective of ice streams that underwent surging activity with comparable landform signatures such as crevasse-squeeze ridges, megaflutings and thrust moraines found at surge-type glaciers Eyjabakkajökull and Bruarjökull in Iceland (Evans, Clark, & Rea, 2008; Evans & Rea, 1999; Russell, 2001; Schomacker, Benediktsson, & Ingólfsson, 2014), Kongsvegen in Svalbard (Bennett et al., 1996; Woodward, Murray, & McCaig, 2002), and Trapridge Glacier in Canada (Clarke, Collins, & Thompson, 1984). These landform assemblages are prevalent in the north and central regions of Alberta.

Fast flow and surging is particularly evident in the cross-cutting relationship between landforms in Alberta formed by the Central Alberta and High Plains Ice Streams (CAIS and HPIS) (Ó Cofaigh, Evans, & Smith, 2010). These cross-cutting landforms indicate complex flow behaviour as the ice sheet began to retreat, and at approximately 16 Cal ka BP the CAIS and HPIS were replaced by another large ice stream, named IS2 by Ó Cofaigh et al. (2010), flowing from the same hypothesised onset zone of the CAIS but in a NW-SE direction, before it shut down at approximately 15.5 Cal ka BP (Atkinson et al., 2014; Margold, Stokes, & Clark, 2018; Ó Cofaigh et al., 2010). These reconstructions highlight the complexities and instability of ice streaming in the southwest LIS. Up until now, flow in this region has not been considered in the context of nearby buried oil sands which occur north of the onset zone of the complex flow behaviour of the CAIS.

Oil sands are highly viscous petroleum products stored within loose or partially consolidated sandstones (Gibson & Peters, 2022). The oil sands are an unconventional heavy crude oil which is viscous

at atmospheric temperature and pressure and is believed to behave as a non-Newtonian shear fluid, meaning viscosity decreases with increasing shear (Bazyleva et al., 2010). The wettability structure of the Alberta Oil Sands (AOS) is also believed to be water-wet, meaning that the sand grains are surrounded by a thin lens of water (nanometric in thickness) which separates the individual grains from the oil (Czarnecki et al., 2005; Neil & Si, 2018). This water-wet property and relatively high porosity makes oil easily extractable from the oil sands deposits using hot water to agitate the oil and separate it from the surrounding sediment (Mossop, 1980). There are three major oil sands deposits in Alberta: (i) the Athabasca, (ii) the Cold Lake and (iii) the Peace River deposits (Figure 1). These deposits lie to the north and east of the reconstructed onset zone of the CAIS and are located anywhere from 70 to 600 m below the surface, although natural exposures of AOS deposits are present along the Athabasca and McKay Rivers. Sediment geochemistry work has also identified transported oil sands deposits in sediments both within and outside of these natural exposure and mining areas (Andriashek, 2018; Andriashek & Pawlowicz, 2002; Fleming et al., 2012; Paragon Soils and Environmental Consulting, 2006). The depth and sediment type in which these hydrocarbons were found meant they could not be linked to anthropogenic extraction, contamination, or even contemporary erosion and deposition; so therefore, they must have been mobilised by historic sediment transport processes such as glacial erosion (Andriashek & Pawlowicz, 2002; Paragon Soils and Environmental Consulting, 2006).

Bituminous erratics (sandstone-bearing oil sands material) and oil sands in till (free hydrocarbons incorporated in till) have also been

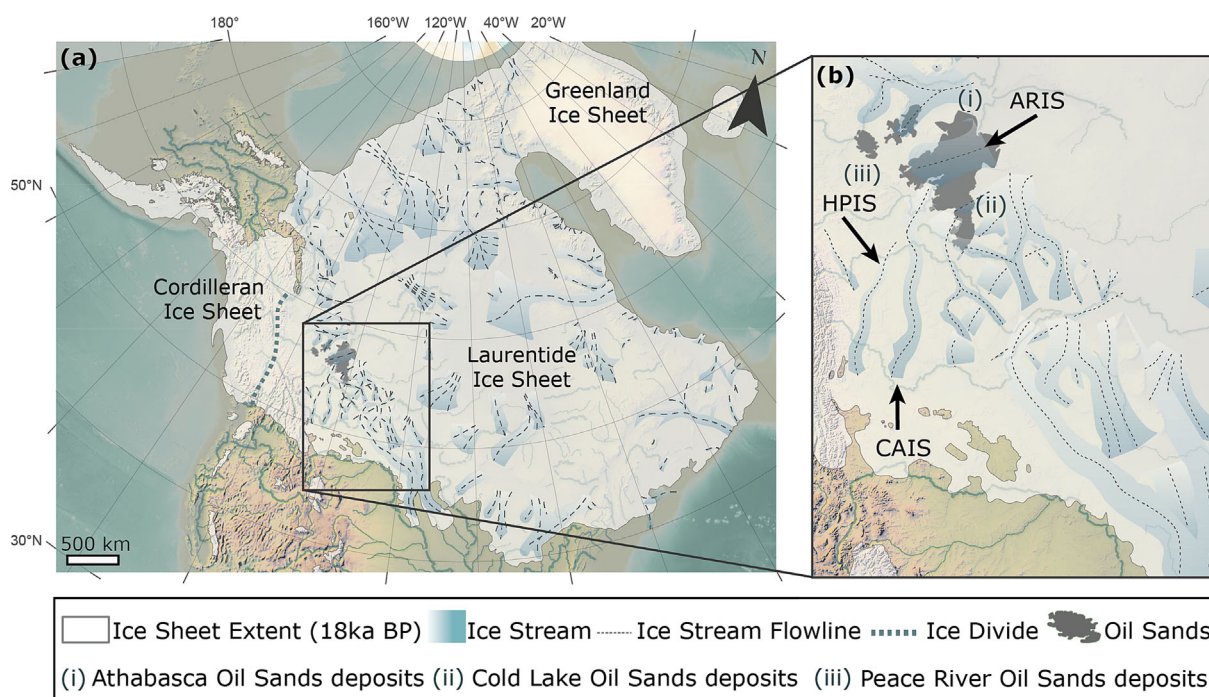


FIGURE 1 (a) Extent of the Laurentide Ice Sheet, Cordilleran Ice Sheet and Greenland Ice Sheet during the LGM at 18 ka BP, from Dalton et al. (2020). Ice streams including the Central Alberta Ice Stream (CAIS), High Plains Ice Stream (HPIS) and Athabasca River Ice Stream (ARIS) (highlighted in the grey box), are drawn after Margold et al. (2015). (b) Region of complex ice streaming in Alberta and Saskatchewan and the location of the CAIS in relation to the AOS deposits drawn after Auch (2014). The CAIS and HPIS are believed to have operated during the LGM, whereas the ARIS and cross-cutting ice streams to the east are deglacial ice streams or of unknown age (Margold et al., 2015). Digital elevation model from © Geospatial Information Authority of Japan and natural earth and bathymetric model from General Bathymetric Chart of the Oceans (GEBCO) grid.

discovered outside of the oil sands region, indicating even more widespread glacial transport. Rutherford (1928) first observed bituminous sandstone boulders in central Alberta, south of the source rock and hypothesised they had been glacially transported. More recent excavations by Tartan Energy Inc (2011 and 2012) also discovered bituminous erratics ~10 km north of Manawan Lake, to the south-west of the Athabasca Oil Sands. Andriashek (2018) compiled evidence of bituminous erratics, bitumen odour and oily sheens in boreholes occurring as far south as Edmonton, as well as oil sands in water well lithologies north of Battle River, and as far south-west as Calgary. More recently, McCerery et al. (2023) hypothesised that glacial erosion and transport processes had eroded and mobilised oil sands deposits from the north of the province and deposited sediments outside of the areas typically associated with natural AOS exposures.

Previous work on the physics of sediment surfaces has shown that oils, such as those found in the AOS, alter the surface chemistry of individual particles—creating a hydrophobic (water repellent) sediment with very limited water infiltration (Gordon et al., 2018; McCerery et al., 2021). The presence of an oil in sediments can also create thin lubricant coatings on the particles that allow for enhanced water shedding, making the sediment ‘slippery’ (McCerery et al., 2021). For this to occur, several other conditions must be met in the sediment system: (i) the primary sediment must be fine-grained (clay-fine sand sized), (ii) the sediment chemistry must preferentially wet one of the lubricants/liquids and (iii) sufficient water delivery is required to sustain lubrication.

The impact of these properties can be observed in Alberta today, where the soil and sediment above transported AOS deposits in the subsoil profile becomes oversaturated because of the hydrophobic effects of the oil below limiting water infiltration. This has resulted in prolonged residence time in the upper soils leading to enhanced plant productivity (Paragon Soils and Environmental Consulting, 2006). Where the transported AOS deposits are near-surface and/or at root-depth, the hydrophobic effect can instead lead to poor plant productivity (Paragon Soils and Environmental Consulting, 2006). Persistent water repellence has been reported in Alberta soils after crude oil spills (Roy & McGill, 2000; Roy, McGill, & Rawluk, 1999). A potential mechanism for this long-lasting effect is the presence of slippery liquid infused porous surfaces (SLIPS), which would be difficult to remediate using traditional methods (McCerery et al., 2021). These contemporary observations of oil presence in the subsurface and a sediment grain size of fine-grained sand clay suggests that the glacial sediment in Alberta meets the necessary conditions for SLIPS. It is therefore conceivable that these properties could drive an instability in the basal sediment by impeding infiltration and reducing basal drag where there is sufficient water delivery, which would enhance glacier sliding and deformation processes.

In this paper, we present two hypotheses: (i) that naturally occurring oil sands hydrocarbon material was incorporated at the ice-bed interface of the CAIS and (ii) that this oil will have enhanced basal slipperiness. The consequence of these hypotheses is that fast flow leading to ice streaming was partly driven by the presence of oil sands material at the ice-bed interface. Our null hypothesis is that the presence of oil sands hydrocarbons at the ice-bed interface will have had no effect on ice flow processes.

To investigate these hypotheses, we studied the complex flow patterns in Alberta in relation to the AOS and their impacts on the ice-bed interface with a focus on the location of the CAIS. We

performed a systematic investigation of the geochemical signature of sediments in the CAIS flow track by applying an oil–oil correlation technique to surficial sediments from within and outside of the CAIS. This allowed us to map AOS presence versus absence through the extent of the ice stream limits, demonstrating the locations at which oil was present at the ice-bed interface during the Laurentide glaciation. The pattern of AOS contaminated sediments was then used to inform theoretical models of ice flow behaviour, based on the impacts of oil at the glacier bed on fast flow.

2 | STUDY AREA

The CAIS is one ice stream that operated within the complex flow pattern of the southwest LIS and lies south of the AOS deposits. The CAIS is believed to have started operating at around 20.5 cal ka BP, after the LIS reached its maximum extent (Margold et al., 2018). The CAIS flow track is approximately 320 km long and 160 km wide at its lobate terminating margin. The flow track is composed of smooth streamlined terrain indicative of fast-flowing ice in a north to south direction, over the flat prairies of central Alberta (Evans, Young, & Cofaigh, 2014). Glacial landform mapping by Atkinson et al. (2014) identified clear landform associations across Alberta. In the north, crevasse-filled ridge sediments and eskers are superimposed on small to medium flutings, whereas in the south, large flutings and mega-scale lineations dominate, before terminating at the Lethbridge moraine (Atkinson et al., 2014). Thin till is recorded along the centre of the ice stream, with only a thin film of sediment overlying bedrock or previously stratified sediments and limited depositional landforms, suggesting ice-bed decoupling and basal sliding dominated in this part of the ice stream (Evans, 2000; Evans et al., 2008; Stokes & Clark, 2003).

3 | METHODS

3.1 | Sediment sampling

Sediment samples were collected using a combination of systematic equal interval transects and sampling of sediment exposures. Transects were constructed using Google Earth software to identify sampling points every 10 km along road transects west to east, across the width of the CAIS (Figure 2). Between 6 and 14 samples were collected across 7 transects, spanning the limits of the CAIS, totalling 66 samples. Samples were taken away from the roadside at shallow depths of 20–50 cm using a shovel and trowel. A further 16 samples were taken from sediment exposures which were identified along the transect using Google Earth imagery and a literature search of glacial landform sedimentology, resulting in a total of 82 sediment samples. When sampling from a sediment exposure, samples were collected approximately 5–10 cm deep into the exposure to limit the impact of oxygenation on the chemical composition of the sediment. Fifty grams of sediment was collected at each site and stored in a sealed 50 mL plastic sample tube. For each exposure, an individual sediment log was constructed where the macroscale properties were recorded for each section of the exposure. GPS coordinates, photographs and sketches were used to map the individual units following standard sedimentological codes (Table 1).

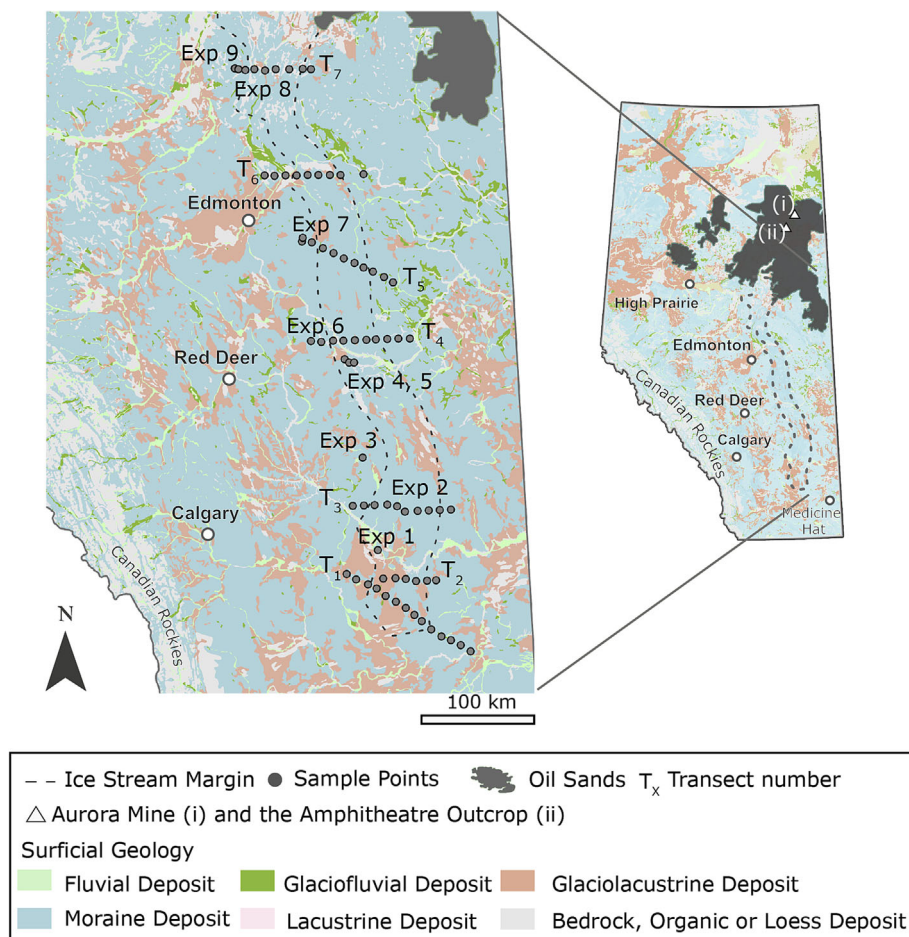


FIGURE 2 Map of Alberta showing the surficial geology and Alberta Oil Sands extent drawn after Alberta Geological Survey, (2003) and Auch (2014); the Central Alberta Ice Stream limits drawn after Margold et al. (2015); and sampling locations on Transects 1–7 and exposures.

3.2 | Petroleum geochemistry

Sediments were freeze-dried for 24 h after which the samples were pulverised to a fine powder. Solvent soluble organic matter was extracted from aliquots (7 g) of the sediment samples using a Dionex™ ASE™ 350 accelerated solvent extractor (ASE) with 90:10, v/v DCM:methanol for 35 min. The extracts were separated into saturated and aromatic fractions using column chromatography, which were then analysed using gas chromatography–mass spectrometry (GC–MS; as per McCerery et al., 2023) on an Agilent 7890B GC fitted with a split/splitless injector (at 280°C) linked to an Agilent 5977B mass selective detector (electron voltage: 70 eV; source temperature: 230°C; quadrupole temperature: 150°C, multiplier voltage: 1800 V; interface temperature: 310°C). The split opened 1 min after the solvent peak had passed, and the GC temperature programme and data acquisition commenced. Separation was performed on an Agilent fused silica capillary column (60 m, 0.25 mm i.d.) coated with 0.25 µm HP-1 phase. The GC was temperature programmed from 50 to 310°C at 5°C/min and held at final temperature for 10 min with helium as the carrier gas (flow rate of 1 mL/min, initial inlet pressure of 50 kPa, split at 30 mL/min).

Diagnostic ratios and compound concentrations used to compare the geochemical signature of the sediments collected from the CAIS were calculated using peak areas quantified on Agilent ChemStation software (Table S1). Individual compound concentrations were semi-quantitatively measured using a relative response factor of one, with internal standards *n*-heptadecylcyclohexane (HDCH) for the saturated compounds and 1,1'-Binaphthyl (1,1-BN) for the aromatic






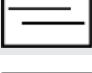

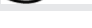
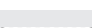
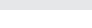
compounds. The key diagnostic ratios, used to distinguish AOS contamination in sediments, outlined in McCerery et al. (2023) were then used to determine geochemical similarities in the sediment samples indicative of AOS contamination (supporting information sections 2.1, 2.2 and 2.3).

3.3 | Data analysis and mapping

The concentrations of two key compounds associated with AOS presence: gammacerane and 28,30-bisnorhopane (BNH) (e.g. Brooks, Fowler, & Macqueen, 1988; Yang et al., 2011) were used to map oil contamination prevalence within and outside the CAIS ice stream limits. The concentrations of gammacerane and 28,30-BNH in each sample were added as vector data points to a GIS database and classified using a Geometric Interval classification method. As both key compounds are terpane biomarkers, a ranking classification was also performed for each sample, based on the key diagnostic ratio values from the sterane, terpane and aromatic hydrocarbon series.

The 12 key indicators of AOS contamination, based on the findings outlined in McCerery et al. (2023), were the following: C₂₉ 14α(H),17α(H) 20S/20R steranes (St29S/R) and C₂₉ 14β(H),17β(H) 20R steranes/C₂₉ 14α(H),17α(H) 20R steranes (St29I/R) from the sterane series, C₃₅ 17α(H),21β(H)/C₃₄ 17α(H),21β(H) hopanes (35αβ/34αβ), gammacerane index, C₂₄ tetracyclic terpane/C₃₀αβ hopane (C₂₄ Tetra/C₃₀αβ Hop), diahopane/normoretane (Dia/NorM), C₂₉Ts/C₂₉ 17α(H),21β(H) hopane (29Ts/C₂₉αβ), and C₂₇Ts/Tm hopanes (Ts/Tm) from the terpane class, and methylphenanthrene Index-2 (MPI-2),

TABLE 1 Symbols and shorthand codes used to describe the sediment exposure lithologies (modified after Miall 1977; Eyles, Eyles, & Miall 1983; Lee 2017; and Slomka & Utting 2018).

Code	Description
	Diamict (d)
	Clay (c)
	Silt (si)
	Sand (s)
	Gravel (g)
	Lamination
	Sharp/planar
	Wavy/undulating
	Erosion
	Gradational
D - - -	Diamict
Dm -	Diamict - matrix supported
D - - (s)	Diamict - sand matrix
D - m	Diamict - massive
S -	Sand
Sm -	Sand - massive
F	Fines
Fm -	Fines - massive

triaromatic steroid TAS C_{27}/C_{28} (20R), TAS C_{26}/C_{28} (20S), and monoaromatic steroid MAS Dia/Reg C_{27} from the aromatic class. The value ranges for each diagnostic ratio was determined by the range of values for the AOS in McCerery et al. (2023). Each sample was then ranked based on its diagnostic ratio value with a maximum score of 12 (Table 2), which would indicate a concentrated AOS sample with little to no alternative hydrocarbon sources.

Key compounds and diagnostic ratio values that are not present or associated with the AOS (but can often be found in gasoline, diesel, crude and lubricating oils or their incomplete combustion products) were also compiled to obtain an alternative hydrocarbon contamination map. These compounds were diasteranes (DiaSt) from the sterane series, absence of gammacerane in the terpane series, the presence of naphthalene, methylnaphthalene, and fluoranthene and the MP/P and Fla/Pyr ratios from the polycyclic aromatic hydrocarbon (PAH) series, and the absence of aromatic steroids. Each sample was ranked based on its diagnostic ratio and the presence/absence of molecular compounds—with a maximum score of 8 (Table 3) indicating an alternative hydrocarbon source with little to no AOS contamination.

The contamination scores were added to the GIS database where all data points were classified using an equal interval classification method to map the likelihood of oil contamination from the AOS and the distribution of other hydrocarbon contamination sources in surficial sediments from the CAIS flow track.

TABLE 2 Biomarker and non-biomarker diagnostic ratio values used to calculate an AOS contamination score.

Diagnostic ratio	Value range	Oil contamination potential score
Steranes		
St29S/R	0.68–0.69	1
St29I/R	0.68–0.71	1
Terpanes		
$35\alpha\beta/34\alpha\beta$	>1.0	1
Gammacerane index	>1.0	1
C_{24} tetra/ $C_{30}\alpha\beta$ hop	0.16–0.23	1
Dia/NorM	0.31–0.41	1
29Ts/ $C_{29}\alpha\beta$ hop	0.57–0.71	1
Ts/(Ts + Tm)	0.22–0.26	1
Aromatics		
MPI-2	0.71–0.78	1
C_{27}/C_{28} (20R)	0.76–0.84	1
C_{26}/C_{28} (20S)	0.36–0.42	1
MAS dia/reg C_{27}	0.22–0.30	1

Note: All ratios were weighted equally and given a rank value of 1.

TABLE 3 Biomarker and non-biomarker key compounds and diagnostic ratio values used to calculate an alternative contamination source score.

Diagnostic ratio	Value range	Alternative source score
Steranes		
DiaSt	<0.1	1
Terpanes		
Gammacerane	Absent	1
Aromatics		
Naphthalene	Present	1
Methylnaphthalenes	Present	1
Fluoranthene	Present	1
MP/P	<2.0	1
Fla/Pyr	>1.0	1
Aromatic steroids	Absent	1

Note: All ratios are weighted equally and given a rank value of 1.

4 | RESULTS

4.1 | Transect sedimentology and geomorphology

The surficial sediments across all seven transects are classified as predominantly glaciolacustrine, glacial moraine and fluvial in origin (Figure 2). The landform associations of the southerly Transects 1–4 are shown in Figure 3. The terminating margin of the CAIS is marked by a major meltwater channel which runs perpendicular to ice flow. Transect 1 sampling was conducted north of this meltwater channel. In this transect, the outer limits of the CAIS are dominated by moraines and crevasse fills, whereas inside the ice stream limits, drumlins and streamlined bedforms running parallel to the ice stream flow are more abundant. A similar pattern is seen in Transect 2, which is

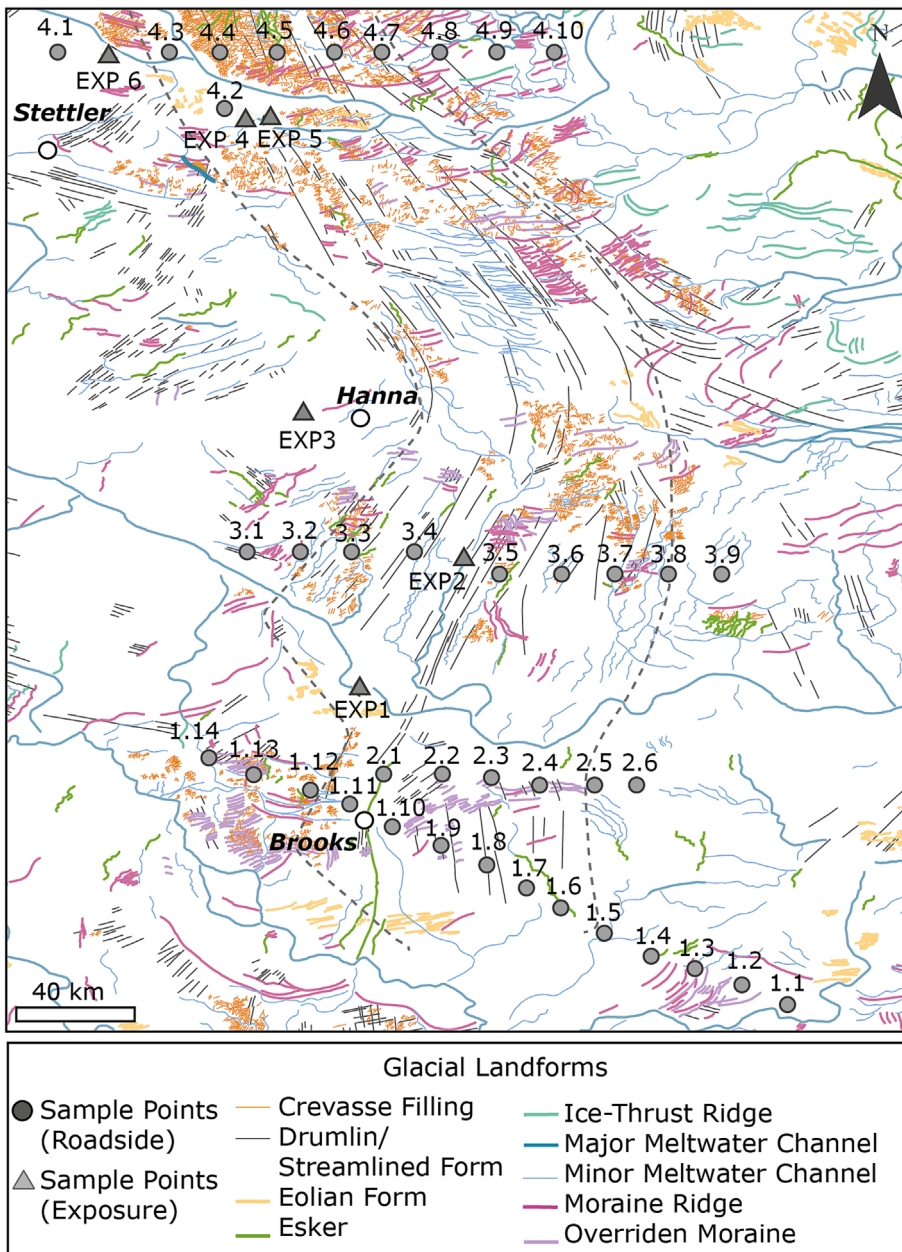


FIGURE 3 Map of surface and exposure sediment sample locations in relation to glacial landforms (drawn after Atkinson et al. 2014), in the southern limit of the ice stream flow track.

located south of the Badlands—a region of heavily eroded bedrock, with few depositional landforms within the ice stream flow track. Exp 1 is located north of Transect 2 and lies south of a major meltwater channel. The exposure face is approximately 4 m high and has been previously characterised as an abandoned river terrace by Berg and McPherson (1972).

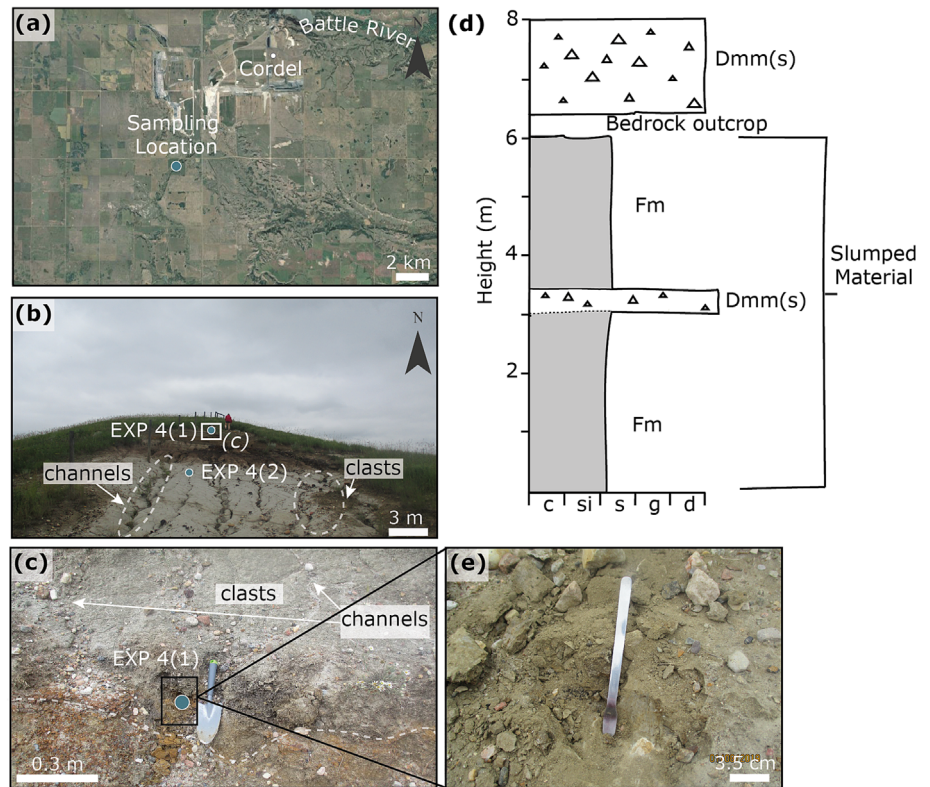
Transect 3 is located in the flat prairies and is also dominated by drumlins and streamlined bedforms inside the ice stream limits. However, there is also a larger number of minor meltwater channels that occur between sample points not seen in the more southerly transects and a number of crevasse fill features to the west and north of the Transect. Exp 2 is approximately 1.5 m high and is cut into the side of a reservoir which has been characterised as a major meltwater channel by Atkinson et al. (2014). Exp 3 to the north of Transect 3 is located outside of the ice stream flow track, and the surrounding landscape is composed of kettle hole landforms with several drumlinoids to the east and aeolian forms to the west. The exposure face is approximately 2 m high and lies in the centre of a moraine ridge that runs perpendicular to the transect and direction of ice flow.

Transect 4 marks a change in the landform assemblages found within the ice stream limit with crevasse fills dominating this part of the ice stream. This transect is also located north of a major meltwater channel that runs perpendicular to ice flow across the full width of the ice stream. Exp 4–6 were also sampled along this transect close to meltwater channels.

Field photographs and interpretations of Exp 4 are shown in Figure 4. A sample was taken from the top-most unit, which is an approximately 2 m thick, well consolidated, yellow/brown, sandy diamict. It contains small clasts (-4 to -5ϕ) which range from sub-rounded to very angular. This unit is also iron rich. Below this is a bedrock outcrop exposed by reworking and slumping of the upper diamict post-deglaciation. A second sample was taken from sediment beneath the bedrock outcrop composed of reworked slumped material from the upper diamict.

Exp 5 is a bedrock outcrop approximately 4.5 m high with a thin surficial sediment layer, located in a minor meltwater channel running parallel to the transect. The sample was taken from the top of the exposure where the sediment layer was thickest. Exp 6 is also located in Transect

FIGURE 4 Field photographs and lithology of Exp 4. (a) The sampling location (52°24'16.62"N, 112°12'13.31"W) south of Cordel and Transect 4. (b, c) Samples were taken from two units overlaying a bedrock bump which is exposed at approximately 6 m; Exp 4(1) was taken from the upper diamict with Exp 4(2) taken from slumped material below the bedrock outcrop. (d) Sediment log of Exp 4 showing the sedimentological units, comprised of diamict and slumped reworked material separated by outcropping bedrock. (e) AOSM in the form of small tar balls found beneath the surface sediment in Exp 4(1). Sediment codes used in the exposure schematic are shown in Table 1. AOSM, aggregated oil sands material.



4 and is a probable crevasse fill based on the narrow morphology and sharp crest, and the surrounding landscape geomorphology. The exposure face is approximately 1.5 m high, south of a minor meltwater channel that runs perpendicular to the transect. To the west of the sampling location, the landscape is composed of Kettle Hole landforms.

The landform associations of the northerly Transects 5–7 are shown in Figure 5. The surrounding landscape of Transects 5 and 6 is characterised by crevasse fill ridges similar to Transect 4, and moraine ridges can also be found close to the ice stream margins. A number of minor meltwater channels parallel to ice stream flow are present outside of the CAIS limits where samples 5.1–5.3 were taken. Exp 7 is located to the west of the transect in the Cooking Lake area of Beaver County (Figure 6). This region is characterised by thick till deposits and Grand Rapids Formation sandstone erratics (Andriashek, 2018; Evans et al., 2008). The exposure is approximately 1.5 m high and stands between several moraine ridges that run perpendicular to the transect. The lower section is approximately 0.5 m high composed of finely laminated, light yellow, poorly consolidated, massive, matrix-supported diamict containing small (–4 to –5 ϕ) subrounded to sub-angular clasts. The lower section has a gradational contact to a 1.5 m high massive, unstructured, dark yellow diamict containing larger (–6 to –7) subrounded clasts.

Transect 6 shows more complex landform assemblages than Transect 5 with a mix of crevasse fill ridges, overridden moraines and minor meltwater channels running perpendicular to flow in the ice stream flow track. A shift to more streamlined landforms and less depositional features is then observed further north into Transect 7. This transect is the closest transect to the AOS deposits to the north and east. Drumlinoid and streamlined landforms running parallel to ice flow dominate the landscape inside the ice stream limits. Exp 8 and 9 were also taken along Transect 7 outside of the CAIS limits. Both exposures are located in an area of high-elevation woodland

north of a minor meltwater channel. Exp 8 is approximately 2 m high and entirely composed of poorly consolidated, matrix-supported, massive diamict. Exp 9 is also 2 m high and entirely composed of poorly consolidated, massive gravel.

4.2 | Visual evidence of Alberta oil sands material

Visual evidence of AOS material (AOSM) was found in sampling pits 4.7, 5.9, 6.6 and in Exp 4 (Figure 7). Visible oil does not appear to be linked to a specific surficial geology type or landform feature, nor were the samples located close to one another. Although bituminous exposures have previously been identified north of these transects along the banks of the Athabasca River (e.g. Akre et al., 2004; Conly, 2001; Headley et al., 2001), no visible bitumen deposits were identified in any of the sampling pits in Transect 7. All other sampling pits across all transects also showed no discernible evidence of concentrated hardened bitumen deposits.

In the sampling pits, the AOSM appears as darkened banding within the sediment, whereas in Exp 4 (Figures 4 and 7), which was the only landform exposure sample to contain evidence of AOSM, the deposits were hardened and crumbled away from the surrounding sediment in concentrated patches. The AOSM in Exp 4 was also visible from the surface as small black speckles (Figure 7a), which were then revealed to be more concentrated deposits upon removal of the most surficial layer (Figure 7b).

4.3 | Spatial analysis of Alberta oil sands indicators

The characterisation of the geochemical signatures of the sediment samples was based on identification of thermally mature biomarker

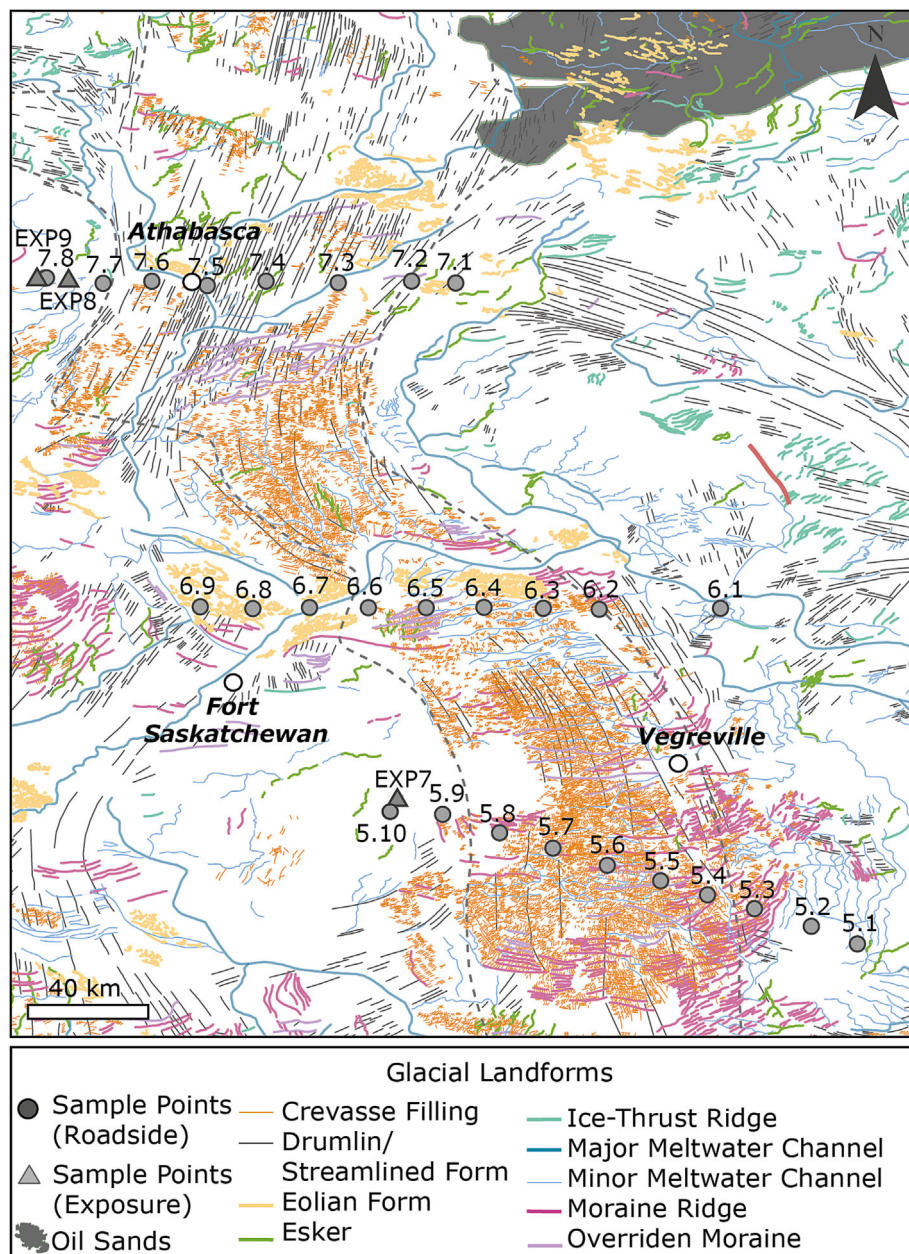


FIGURE 5 Map of surface and exposure sediment sample locations in relation to glacial landforms (drawn after Atkinson et al. 2014) in the northern limit of the ice stream flow track.

signatures from the GC–MS chromatograms. Mature biomarkers are indicative of a petroleum or pyrogenic hydrocarbon source, such as the AOS, and are not typically associated with contemporary sediments and more recent biological material. Samples were then analysed using biomarker and non-biomarker diagnostic ratios and compared to the AOS values measured by McCerery et al. (2023) to identify glacially mobilised deposits (Figures S1–S3).

Firstly, the concentration of two key compounds—gammacerane and 28,30-BNH—were mapped (Figure 8a,b). Both compounds are ubiquitous in AOS deposits (Andriashek & Pawlowicz, 2002; Bennett, Jiang, & Larter, 2009; Brooks et al., 1988; Yang et al., 2011). Secondly, each sample was then assigned an AOS contamination score, based on a diagnostic ratio factor analysis (Figure 8c). Samples 4.4 and 6.3 contained the highest contamination scores, each recording values of 7 out of a possible 12. Samples 4.7 and 6.6, which contained visual evidence of AOSM, were assigned a score of 5, whereas samples Exp 4(1) and 5.9 (which also contained visual evidence of deposits) were assigned scores of 3 and 2 respectively, highlighting the large

influence of alternative contamination on the geochemical signature of the samples. It was therefore deemed that 28% of samples with scores 5–7 have a high likelihood of AOS contamination, 47% of samples with scores of 3–4 have a moderate likelihood and 25% of samples with scores of 1–2 have a low likelihood of AOS contamination.

Thirdly, to account for mixed hydrocarbon signatures, alternative petrogenic and pyrogenic hydrocarbon sources were also mapped (see Figure 8d). An alternative hydrocarbon score was calculated for each sample based on the occurrence of key compounds and diagnostic ratios found in other sources of hydrocarbons, for example, gasoline, diesel, lubricating oil, crude oil and the incomplete combustion products of these and other organic matter—which are not found in the AOS (Figure 8d). The highest alternative contamination scores were in samples 3.2, Exp 6, 4.6, 4.9, 7.6, and 7.8, which each scored 6 out of a possible 8.

Based on these results, the samples can be broadly grouped into the following four categories:

FIGURE 6 Field photographs and lithology of Exp 7. (a) The sampling location (53°23'46.29"N, 112°46'52.89"W) near Lindbrook on Transect 5. (b, c) The four sampling locations on the exposure. The contact between the two sedimentological units is highlighted by the white dashed line. (d) The exposure is composed of two distinct sedimentological units, both comprised of sandy diamict with clasts. (e) Laminations in the lowest sedimentological units. (f) Clasts are subrounded to subangular, decreasing in abundance from the top to the bottom of the exposure. The sediment codes used in the exposure image are shown in Table 1. Although visual evidence of AOSM was not found in Exp 7, the sediment sample from the till was originally analysed in McCerery et al. (2023), where it showed a geochemical signature indicative of AOS contamination. AOS, Alberta Oil Sands; AOSM, aggregated oil sands material.

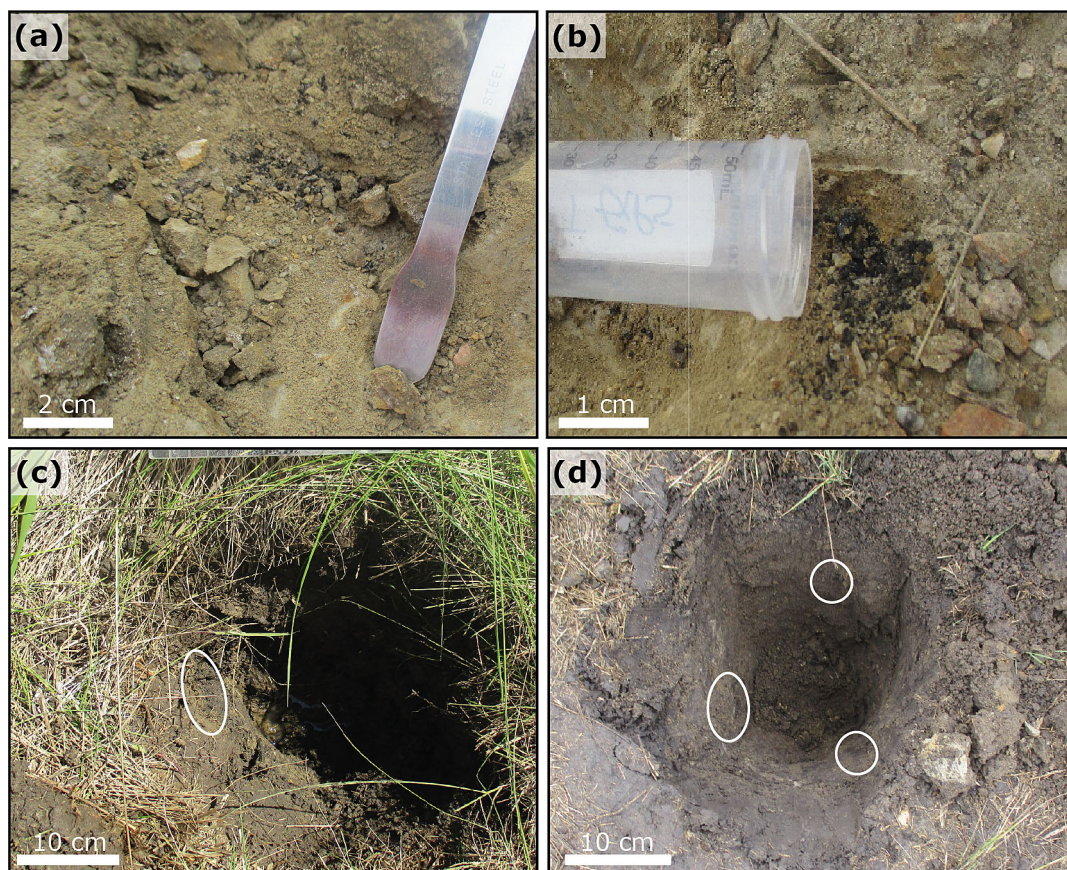
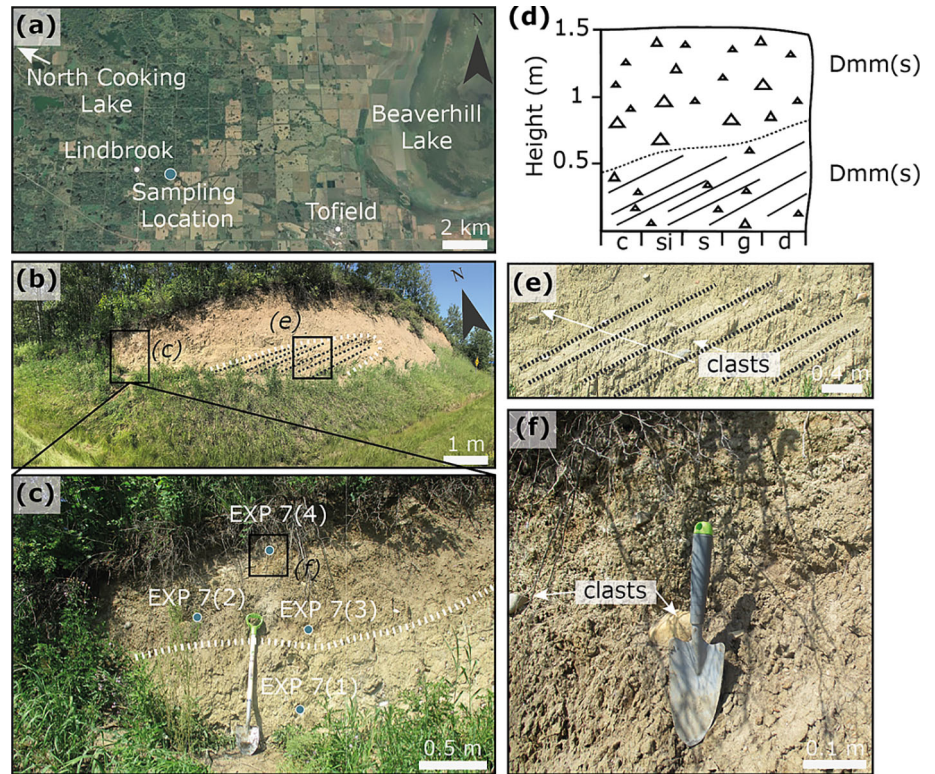


FIGURE 7 Field photographs of aggregated oil sands material (AOSM), highlighted by white circles, in sediment sampling pits. (a) Small accumulations of AOSM at the surface where sample Exp 4(1) was taken. (b) Larger accumulations of AOSM beneath the surface where sample Exp 4(1) was taken. (c) Dark bands of AOSM at the subsurface where sample 5.9 was taken. (d) Dark bands of AOSM at the subsurface where sample 6.6 was taken.

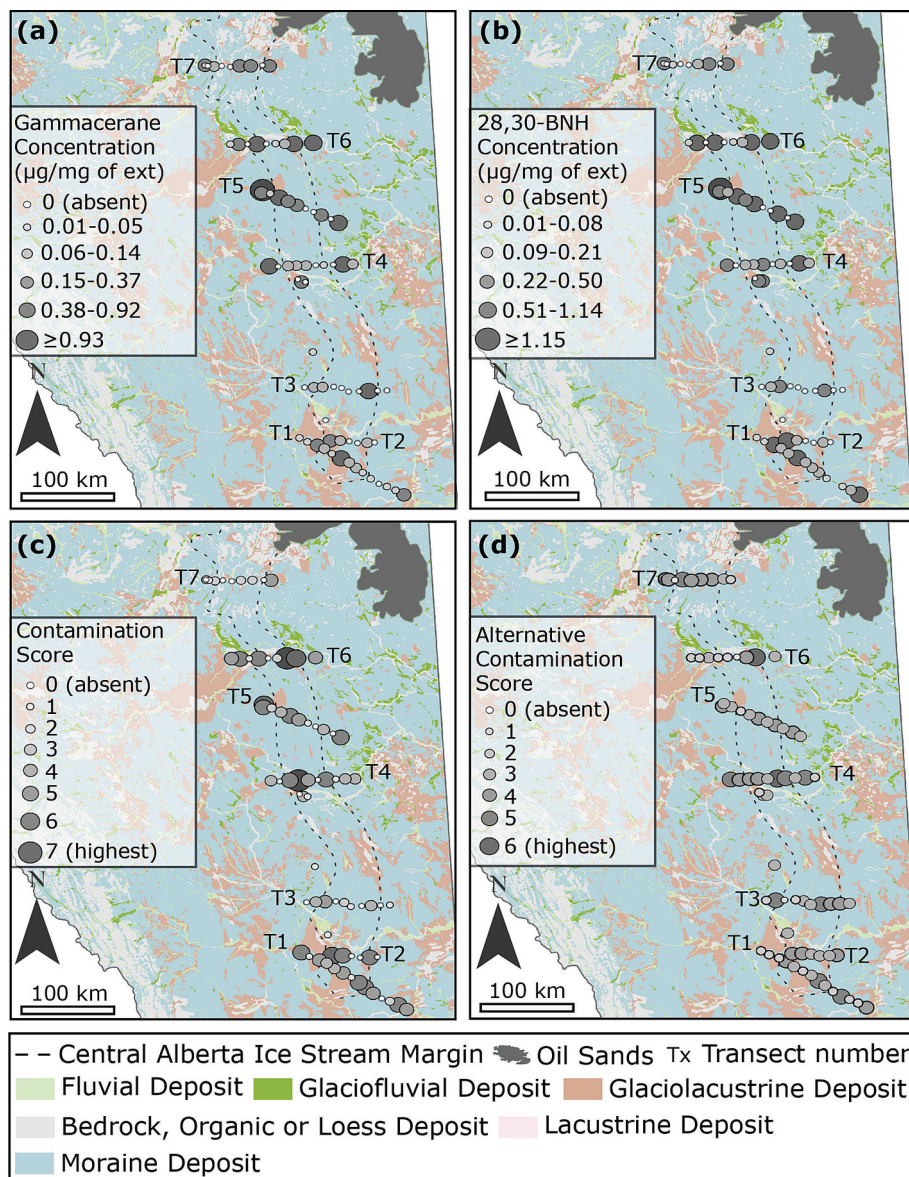


FIGURE 8 Maps of key biomarker compounds within and outside the Central Alberta Ice Stream (limits identified by Margold et al. 2015). Graduated symbol map of (a) the concentration of gammacerane and (b) 28,30-bisnorhopane of the total extracts. (c) Graduated symbol map of the AOS contamination score and (d) alternative contamination score. The AOS extent was drawn after Auch (2014) and the surficial geology from the Alberta Geological Survey (2013). AOS, Alberta Oil Sands.

1. Sediments that have been contaminated with AOS and show little indication of an alternative hydrocarbon source.
2. Sediments that have been contaminated with AOS but also show substantial alternative hydrocarbon contamination.
3. Sediments that have a low likelihood of AOS contamination and show substantial alternative hydrocarbon contamination.
4. Sediments that have a low likelihood of AOS contamination and show little indication of an alternative hydrocarbon source.

The samples which have high concentrations of gammacerane and 28,30-BNH, high AOS contamination scores, and returned low values for the alternative hydrocarbon contamination scores were 1.2, 1.14, 2.5, 5.1, 6.6, Exp 7(2) and Exp 7(3). These samples are found in the south and east of Edmonton in the CAIS flow track. Their geochemical signature can be attributed to the AOS because of the presence of key indicator compounds, high similarities in diagnostic ratios and low indication of alternative hydrocarbon mixing. Of these samples, only sample 6.6 had clear visual evidence of AOSM in the field.

Most of our samples returned a mixed hydrocarbon signature and fall within the second category of having potential AOS and another petrogenic/pyrogenic hydrocarbon contamination (including samples

that had visual evidence of AOSM, 4.7, Exp 4(1) and 5.9). These samples are found throughout the full extent of the CAIS flow track. The highest AOS contamination scores (5–7) were calculated in samples 1.6, 1.7, 2.1, 2.2, 4.3, 4.4, 4.7, 5.7, 5.10, 6.2 and 6.3, indicating long-distance transport of the oil sands deposits.

The other samples that have a mixed signal show a more complex geochemical signature, likely because of higher concentrations of immature contemporary inputs such as terrestrial plant matter, and a mixture of other petrogenic and pyrogenic hydrocarbon sources. Where the AOS contamination scores are moderate or low and the alternative hydrocarbon sources are ≤ 3 , the signature cannot be confidently attributed to the AOS, but they do share some of the key indicators. This does not completely exclude the AOS as a contamination source in these samples. For example, visual evidence of AOSM was found in the sampling pits of samples 5.9 and Exp 4(1) (despite having a contamination score of 2 and 3, respectively), which could be because of the geochemical influence of surrounding sediments and contaminants affecting the diagnostic ratios. The source of the alternative contamination in most samples is a combination of petrogenic and pyrogenic sources of PAHs, evidenced by the presence of PAHs fluoranthene and phenanthrene which are not associated with the

AOS. This suggests that their organic geochemical signature is a mixture of AOS and an alternative contamination source.

The alternative contamination scores also allowed for the identification of samples that have been contaminated with hydrocarbons unrelated to the AOS. Samples 1.4, 3.6, 3.8, 4.6, Exp 6, 5.4 7.3, 7.4, 7.5, 7.6, 7.8 and Exp 9 scored as absent or unlikely (0–2) in the AOS contamination score but highly on the alternative contamination source score (4–6), indicating an alternative hydrocarbon source as the dominant or only source of hydrocarbons in those samples. The majority of these samples are concentrated in the northernmost transect, Transect 7 which is located closest to the ice stream onset zone and AOS deposits, whereas samples 1.3, 1.13, Exp 3(3), Exp 7(4), 6.4, 6.5 and 7.7 scored as absent or unlikely (0–2) in the AOS contamination score, and low on the alternative contamination source score (1–2). This indicates minimal mature hydrocarbon contamination.

5 | DISCUSSION

The geochemical signature of AOS found within the CAIS flow track, south of the known AOS limits, proves our first hypothesis that oil sands material was incorporated at the ice-bed interface during the Laurentide glaciation. The heterogeneous pattern of deposits reflects two potential processes, (i) as we do not expect a uniform oil layer to be present through the full extent of the CAIS, the pattern of AOS contamination reflects the different locations of deposition. This is also supported by the visual evidence of AOSM in some sampling pits but not all. (ii) The geochemical signature is also degraded overtime after thousands of years of biodegradation, exposure and reburial, and in some areas the signature could also be masked by contemporary signatures from other contaminants and biogenic hydrocarbons from plant material. Because of the time elapsed since deposition, progressive burying and the effects of biodegradation, it was not likely we would see extremely strong uniform AOS-only signatures across the CAIS. This pattern of AOS signatures reveals that glacial processes eroded and transported oils from the very north of the ice stream to its southern limit. The geographical extent of the AOS geochemical signature we record here further supports the reports of oil sands in water well lithologies as far south as Calgary (as detailed by Andriashek, 2018). This study and the results of other sediment analysis work in Alberta (e.g. Andriashek, 2018; Andriashek & Pawlowicz, 2002; Fleming et al., 2012; Paragon Soils and Environmental Consulting, 2006) suggest that AOSM was spatially extensive and could therefore have a conceivable impact on the sediment properties and subglacial processes occurring at the ice-bed interface during the Laurentide glaciation.

5.1 | Oil sands deposits and geomorphology

There is an interesting question as to whether the pattern of AOS signature is linked to surficial geology and geomorphology in Alberta. Figure 8 shows the pattern of increasing occurrence of an AOS signature in sediments coincides with areas of thick till deposits found in the north and south of the ice stream flow track covering Transects 1–2 and 4–6. Areas with lower AOS signatures coincide with regions of thin till cover through the centre (Transect 3) and most northerly

transect (Transect 7). This is particularly apparent in Transect 3, which covers the Badlands, where there is a weak or absent oil signature in most of the samples. This is an area of thin till cover which has previously been linked to ice-bed decoupling or subglacial deformation processes by Evans and Campbell (1992) and Evans et al. (2008).

Areas of thicker till and increased AOS signature are found in areas dominated by depositional landforms inside of the ice stream limits. In Transects 4 and 5, there are a large number of moraine and crevasse fill complexes close to samples 4.4 and 5.7 which have high AOS contamination scores (Figures 3 and 5). In comparison, the areas with less depositional landforms, such as Transects 3 and 7, which are dominated by streamlined forms, have a lower AOS contamination score. This suggests that oil-laden sediments were transported and not deposited through parts of the ice stream and so do not appear in the sediment geochemistry of streamlined bedforms. Therefore, the retained AOS signature may be linked to areas of deposition in the ice stream flow track. Work on crevasse squeeze ridges have previously suggested that sediments from the ice-bed interface are retained in the ridges as flow decelerates (Woodward et al., 2003). Similar focusing of AOS signature in Albertan landforms may reflect such a process.

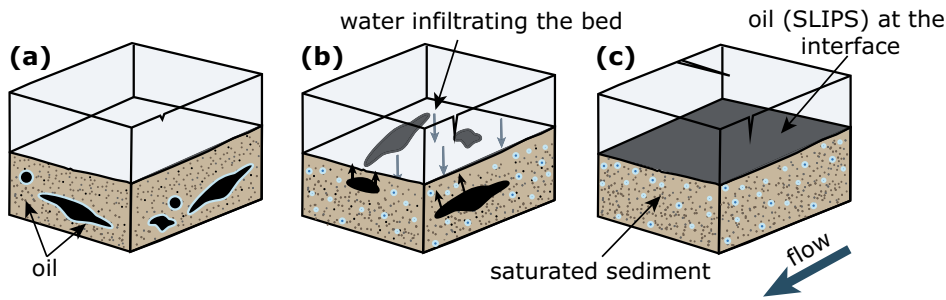
5.2 | The effect of oil on ice flow processes

The hydrocarbon geochemical similarity of the surficial sediments to oils in Northern Alberta demonstrates oil sands deposits were eroded and mobilised from the north, near the onset zone of the CAIS. Based on the surficial geology type of the province and the observations of bitumen in glacial sediment sequences by Andriashek and Pawlowicz (2002), Paragon Soils and Environmental Consulting (2006), Fleming et al. (2012), and Andriashek (2018) as well as this study, a glacial origin for the mobilisation of these deposits is most likely.

We hypothesise that as AOS deposits were exposed through gradual erosion of surface sediment and incorporation of subglacial meltwater, oil would be freed from the surrounding sandstone. The subsequent continual erosion would lead the oils to become mobilised within the till at the bed of the CAIS and travel along the ice-bed interface, before being deposited by slower-flowing ice or glacial meltwaters.

Existing work on the physics of interfaces has shown that oils such as the AOS can alter the surface chemistry and lubricating interface of surfaces and sediments (Gordon et al., 2018; McCerery et al., 2021). McCerery et al. (2021) showed that microscopic layers of oil are required to exert such effects on fine sediment particles. This therefore supports our second hypothesis that the incorporation of AOS at the ice-bed interface will have enhanced slipperiness. In the case of the AOS, the sediment is water-wettable and so incorporation of even small amounts of an oil into the sediment will create a lubricating water–oil interface, similar to the SLIPS system in the *Nepenthes Pitcher Plant* (Wong et al., 2011). These surfaces are highly water-shedding and slippery and would influence the physics driving basal sliding and deformation if they were to occur at the ice-bed interface. It is therefore possible to envisage two scenarios whereby oil sands deposits with water-wettable sediment could form slipperiness at the bed of the CAIS through erosion and mobilisation (Figure 9).

1. Macroscale SLIPS - water-wet behaviour



2. Microscale SLIPS

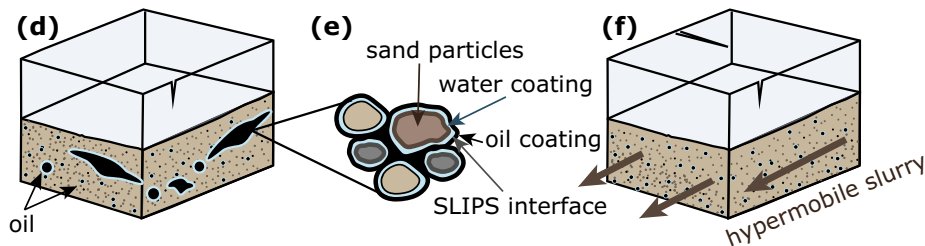


FIGURE 9 Schematic diagram of two hypothesised slippery scenarios at the bed of an ice stream or glacier because of oil–water interfaces. In the first model, (a) water-wet oil sands deposits occurring within the basal sediments are gradually eroded by glacial action (b) exposing the oil to the ice–bed interface. (c) The water-wet nature of the sediment means it is preferentially wetted by water, resulting in an oil–water liquid–liquid interface and reduced water infiltration into basal sediments. In the second model, (d, e) the oil sands deposits are water-wet and create a water–oil interface between the individual sediment particles; (f) under pressure from the overlying ice, the sediment bed forms a hypermobile slurry between the individual grains.

5.2.1 | Macro-scale SLIPS

In the first scenario, a macro-scale SLIPS would form where the gradual erosion of the substrate exposes the oil deposits below the ice (Figure 9a–c). As the oil is gradually exposed at the ice–bed interface, a SLIPS would form at the oil–water contact of the warm bedded ice stream. Based on the spatial distribution of oil deposits in the CAIS, it is likely that once exposed the oil is then partly mobilised at the interface before being deposited in parts of the ice stream.

At the ice bed, further water infiltration is impeded because of the hydrophobicity of the AOS, increasing basal water pressure and enhancing glacier sliding. Here, an oil saturated layer at the ice–bed interface would act in a similar way to an impermeable bed. A similar process is proposed to have operated in the region because of the presence of soft clay-rich sediments which would swell when saturated and become locally impermeable (e.g. Clayton, Teller, & Attig, 1985; Evans et al., 2014). The poor drainage in both of these cases results in an increase in basal water pressure which could result in localised ice–bed decoupling and fast sliding.

5.2.2 | Micro-scale SLIPS

In the second scenario, a micro-scale SLIPS would form where the slipperiness occurs between individual grains (Figure 9d–f), rather than at the larger scale between the ice–bed interface. In this model, the water-wet AOS deposits are composed of individual sand grains coated in a thin layer of water separating it from the oil. The oil and immiscible water reduce the amount of solid contact between the individual grains, making them ‘slippery’. Under the pressure of an overlying glacier or ice sheet, and facilitated by delivery of water to the bed, this could create a microscale SLIPS with individual grains moving over one another because of the oil–water interface. If this is widespread, there is a potential to create a hypermobile slurry at the glacier bed (similar to a debris flow), which would enhance basal

deformation and drive fast flow of the ice above. This behaviour is even less stable than that of a dilated, deforming till, where the decrease in grain contact occurs through an increase in pore water pressure (e.g. Evans et al., 2006). In the micro-SLIPS case, till grain contact is already low (because of the presence of the oil and liquid film) and therefore requires less water infiltration and pressure to initiate the deformation process. A SLIPS hypermobile slurry is also analogous to Phillips et al.’s (2018) theory of deforming till liquefaction in response to icequakes. In Phillips et al.’s (2018) theory, the energy exerted on subglacial saturated sediments during a seismic event cause the sediment to become liquified in order to release the pressure of the intergranular porewater. This process, in the same way as the micro-SLIPS, promotes clast and grain flow which creates a ‘transient mobile zone’ at the sediment bed, aiding soft bed sliding.

5.2.3 | Implications of models

These models are a potential explanation for why the position of the onset zones of complex and fast flowing ice streams coincide with the AOS deposits in Northern Alberta. The incorporation of oil sands into glacial sediment will inevitably influence the physical properties of the interface in the subglacial environment and therefore impact the location of fast flow. This builds on the existing mechanisms for fast flow and unstable behaviour in this region such as the deformation of soft sediments (e.g. Clark, 1994; Evans et al., 2014; Eyles, Boyce, & Barendregt, 1999) and adds a further sediment characteristic that would influence flow conditions.

The gradual erosion and mobilisation of oils through the bed of the CAIS will therefore have also influenced some of the surging behaviour. Because of the stratigraphy of the AOS deposits (Mossop, 1980), a constant supply of oil to the glacial environment would not be expected. As rates of erosion and deposition would result in cyclical exposure of oil sands and mobilisation at the ice–bed interface, a cyclical impact on glacier flow might occur. As oils are

removed by erosion, resulting in fast flow, their subsequent deposition would result in a halt in this behaviour until new oils are exposed from the deposits in the north. These transitions between a fine-grained permeable sediment bed where no oil is present at the interface, and an impermeable oily bed when oil is exposed would result in shifts in dominant flow regimes and temporal variations in flow speed. This would simulate spatial flow transitions from a permeable 'sticky' sediment on the upstream end of ice stream flow to an oily 'slippery' sediment downstream of the AOS where a shift in geochemistry and the presence of a lubricating interface occurs. Furthermore, the surface elevation changes associated with fast flow and ice thinning in the oily bed regions could have also influenced the ice stream positioning during deglaciation. The fast flow experienced in the CAIS may have resulted in fast thinning which could have contributed to the nearby ice stream positions, alongside other drivers such as proglacial lake drainage, changing thermal regime, and shifting of the ice divides (e.g. Margold et al., 2018; Norris et al., 2018; Ó Cofaigh et al., 2010; Utting & Atkinson, 2019), thus leading to the complex cross-cutting patterns.

5.3 | Implications for other palaeo ice streams and ice sheets

Because of their proximity to the AOS, it is possible that the HPIS and Athabasca River Ice Stream (ARIS) also experienced enhanced sliding and deformation processes associated with incorporation of oils into basal sediment. The ARIS in particular operated directly over the AOS and therefore likely contributed to the erosion and exposure of AOS to the ice-bed interface of the ice sheet. However, as described previously, there are a number of conditions that need to be met in order for a SLIPS model to apply in the glacial system, such as (i) the primary sediment size, (ii) pre-existing sediment chemistry and (iii) sufficient water delivery to sustain lubrication. It should therefore be noted that the Interior Plains also experienced ice streaming outside of the AOS limits, particularly in Saskatchewan (i.e. Saskatchewan River, Maskwa, Lac La Ronge, and Buffalo Ice Streams), that may not be related to the position of the AOS, nor do we seek to explain every ice stream position with SLIPS presence. The pattern of cross-cutting ice streaming is believed to have been initiated on soft sediment by subglacial deformation (Norris et al., 2018). The extreme reorganisation of flow in this region was attributed to shifts in spatio-temporal thermal regimes during ice sheet retreat, changing ice divides and an increase in topographic control associated with ice thinning (Margold et al., 2018; Norris et al., 2018; Ó Cofaigh et al., 2010). We propose that the chemical and physical micro-scale processes occurring within and between sediment particles at the ice-bed interface may also be driving some of the larger dynamics in the subglacial environment in the region surrounding the AOS deposits.

It is therefore likely that similar processes could have occurred beneath other palaeo ice sheets overlying oil deposits as well as in contemporary glacial environments where an oil or other lubricating substance is able to enter the glacial system. For example, in the Barents Sea, loading and unloading of the Pliocene-Pleistocene ice sheets resulted in the tilting and rerouting of hydrocarbon stores and pathways causing hydrocarbon leakages into marine sediments (Fjeldskaar & Amantov, 2018; Fjeldskaar & Kjemperud, 1992; Løtveit,

Fjeldskaar, & Sydnes, 2019). Glacial erosion during this period contributed to releasing oil from shallow depths of the hydrocarbon reserves and also resulted in release of gas hydrates (Kishankov et al., 2022). Erosion and uncapping of these hydrocarbon reservoirs by glacial action have resulted in persistent gas release and oil slick spots (Serov et al., 2023). It is therefore likely that changes to sedimentary basins could have mobilised oils and gases in other glaciated areas of hydrocarbon reserves around the world, both onshore and offshore. Visible oil seeps have been detected and mapped at outcrops along the coast of Greenland, for example (e.g. Bojesen-Koefoed et al., 2007; Christiansen et al., 2020; Christiansen & Bojesen-Koefed, 2021). The extent of these seeps suggests that petroleum deposits are common in Greenland's onshore sedimentary basins (Christiansen & Bojesen-Koefed, 2021). However, these deposits have not yet been considered or explored in the context of glaciation and glacial mobilisation.

Further work is required to fully reject our null hypothesis that oil sands hydrocarbons at the ice-bed interface will have had no effect on ice flow processes. However, currently the geochemical results described here and the physics principles of slippery surfaces mean we also cannot reject our hypothesis that this oil will have enhanced slipperiness at the bed and the implications of this exerting control on ice streaming. To fully prove this paradigm, further work is needed to expand the suite of study sites and identification criteria used to diagnose sediment SLIPS and oil-driven fast flow. Locally, more research on nearby ice streams to show that the AOSM was present in other ice streams in the complex flow pattern region of the southwest LIS would add support to our hypothesis that the ice streams in this part of the LIS were partly driven by the lubricating effect of the oils. Further geochemical analysis of ice streams beyond this area of complex flow to show a lack of AOS signature in sediments in neighbouring ice streams with more conventional flow patterns would add a further control and support our hypothesis that the AOS will have some effect on ice stream flow. This work has highlighted the role glacial erosion has historically played in mobilising hydrocarbons and how these hydrocarbons can impact sediment properties. This extends beyond the scope of the LIS and could affect or have affected glaciations around the globe where hydrocarbon reservoirs underlie glaciers and ice sheets. It would therefore be valuable to perform similar geochemical analysis on sediments from other sites close to hydrocarbon reservoirs such as sediments from the Barents Sea to look for similar erosion and fast flow processes.

6 | CONCLUSION

In this paper, we set out to test two hypotheses. Our results support our first hypothesis that naturally occurring oil sands hydrocarbon material was incorporated at the ice-bed interface of the CAIS, illustrated by the presence of AOS deposits detected across the full extent of the CAIS flow track. The pattern of deposition showed stronger AOS signatures with higher concentrations in the southern limits and east of Red Deer and Edmonton where glacial deposition and depositional landforms such as crevasse fills and moraine complexes dominate the landscape. The lowest concentrations of AOS contamination were found in the centre and most northern limits of the ice stream where thin till cover and streamlined bedforms are more typical. This pattern of contamination may

indicate a link between glacier erosion and deposition and oil sands incorporation in till. This is the first example of long-distance glacial transport of an oil at the ice-bed interface of an ice stream or glacier.

Existing principles of interface physics and the onset zone of complex and unstable fast flow in the former CAIS coinciding with the AOS deposits in Northern Alberta support our second hypothesis that the incorporation of AOS at the ice-bed interface will have enhanced slipperiness. Here, we propose that the unstable and fast flow behaviour could be explained by oil sands incorporation into glacial sediment, as the widespread transport of oils with lubricating properties through the ice stream flow track would affect the conditions at the ice-bed interface. Two models of oil incorporation in basal sediments show that both enhanced sliding and basal deformation could occur because of the presence of an oil-rich sediment-SLIPS. In both models, the creation of an oil-water interface lubricating the bed would enhance sliding by reducing basal drag and driving basal deformation by creating super slipperiness between individual sediment particles (potentially forming a hypermobile slurry). This work highlights the importance of considering sediment geochemistry and the microscale processes occurring at the ice-bed interface for glacier flow instability. By furthering our understanding of the processes acting on the microscale, we can better understand the driving forces of glacier sliding and basal deformation.

ACKNOWLEDGEMENTS

This research was funded by Northumbria University Research Development Fund. The authors would also like to thank Northumbria University for fieldwork and logistical support and Newcastle University School of Natural and Environmental Sciences for laboratory training and access to analytical facilities.

AUTHOR CONTRIBUTIONS

Rebecca McCerery was involved in conceptualisation, methodology, investigation, writing of initial drafts and editing of the manuscript. John Woodward was involved in conceptualisation, funding acquisition, methodology, resources, supervision, and reviewing and editing of the manuscript. Kate Winter was involved in conceptualisation, methodology, investigation, supervision, and reviewing and editing of the manuscript. Onoriode Esegbe was involved in methodology, investigation, resources, and reviewing and editing of the manuscript. Martin Jones was involved in methodology, resources, supervision, and reviewing and editing of the manuscript. Glen McHale was involved in conceptualisation, supervision, and reviewing and editing of the manuscript.

ACKNOWLEDGEMENTS

The authors would also like to thank Northumbria University for fieldwork and logistical support and Newcastle University School of Natural and Environmental Sciences for geochemical laboratory training and access to analytical facilities.

CONFLICT OF INTEREST STATEMENT

No conflict of interest to declare.

DATA AVAILABILITY STATEMENT

Data are available as supporting online information.

ORCID

Rebecca McCerery  <https://orcid.org/0000-0001-6520-3667>

REFERENCES

- Ahmed, A.S., Webster, L., Pollard, P., Davies, I.M., Russell, M., Walsham, P., Packer, G. & Moffat, C.F. (2006) The distribution and composition of hydrocarbons in sediments from the Fladen Ground, North Sea, an area of oil production. *Journal of Environmental Monitoring*, 8(2), 307–316. Available from: <https://doi.org/10.1039/b512616a>
- Akre, C.J., Headley, J.V., Conly, F.M., Peru, K.M. & Dickson, L.C. (2004) Spatial patterns of natural polycyclic aromatic hydrocarbons in sediment in the lower Athabasca River. *Journal of Environmental Science and Health, Part A*, 39(5), 1163–1176. Available from: <https://doi.org/10.1081/ESE-120030301>
- Alberta Geological Survey. (2013) *Surficial geology of Alberta, generalized digital mosaic*. Alberta, Canada: Alberta Energy Regulator/Alberta Geological Survey. Available at: arcgis.com/home/item.html?id=745bb49973194f46b19d5ad2f84afd61.
- Andriashek, L.D. (2018) On the origin of oil sand and related bedrock erratics in glacial sediments of Central Alberta. In: *Alberta energy regulator/Alberta geological survey, AER/AGS Open File Report 2018-13*. Alberta, Canada: Alberta Energy Regulator/Alberta Geological Survey, p. 42.
- Andriashek, L.D. & Pawlowicz, J. (2002) Observations of naturally occurring hydrocarbons (bitumen) in quaternary sediments, Athabasca oil sands area and areas West, Alberta. In: *Alberta Energy and Utilities Board/Alberta Geological Survey, Geo-Note*. Alberta, Canada: Alberta Energy Regulator/Alberta Geological Survey.
- Atkinson, N., Utting, D.J., Pawley, S.M. & Trenhaile, A. (2014) Landform signature of the Laurentide and Cordilleran ice sheets across Alberta during the last glaciation. *Canadian Journal of Earth Sciences*, 51(12), 1067–1083. Available from: <https://doi.org/10.1139/cjes-2014-0112>
- Auch, T. (2014) *Potential extent of Athabasca oil sands*. Ohio, United States: Ted Auch. Available at: www.Arcgis.Com/Home/Item.Html?id=cf6eb687c5394f489ca7321f2dceb4ce, <https://www.arcgis.com/home/item.html?id=cf6eb687c5394f489ca7321f2dceb4ce>
- Bazyleva, A.B., Hasan, A.M.D., Fulem, M., Becerra, M. & Shaw, J.M. (2010) Bitumen and heavy oil rheological properties: reconciliation with viscosity measurements. *Journal of Chemical & Engineering Data*, 55(3), 1389–1397. Available from: <https://doi.org/10.1021/jc900562u>
- Bennett, M.R., Hambrey, M.J., Huddart, D. & Ghienne, J.F. (1996) The formation of a geometrical ridge network by the surge-type glacier Kongsvegen, Svalbard. *Journal of Quaternary Science*, 11(6), 437–449. Available from: [https://doi.org/10.1002/\(SICI\)1099-1417\(199611/12\)11:6<437::AID-JQS269>3.0.CO;2-J](https://doi.org/10.1002/(SICI)1099-1417(199611/12)11:6<437::AID-JQS269>3.0.CO;2-J)
- Bennett, B., Jiang, C. & Larter, S.R. (2009) Identification and occurrence of 25-norbenzohopanes in biodegraded bitumen from Palaeozoic carbonates in northern Alberta. *Organic Geochemistry*, 40(6), 667–670. Available from: <https://doi.org/10.1016/j.orggeochem.2009.04.001>
- Berg, T. & McPherson, R. (1972) *Surficial Geology Medicine Hat (NTS 72L), Technical report*. Alberta, Canada: Alberta Energy Regulator/Alberta Geological Survey. Available at: <https://searchworks.stanford.edu/view/4486865>
- Bojesen-Koefoed, J.A., Bidstrup, T., Christiansen, F.G., Dalhoff, F., Gregersen, U., Nytoft, H.P., et al. (2007) Petroleum seepages at Asuk, Disko, West Greenland: Implications for regional petroleum exploration. *Journal of Petroleum Geology*, 30(3), 219–236. Available from: <https://doi.org/10.1111/j.1747-5457.2007.00219.x>
- Brooks, P.W., Fowler, M.G. & Macqueen, R.W. (1988) Biological marker and conventional organic geochemistry of oil sands/heavy oils, Western Canada basin. *Organic Geochemistry*, 12(6), 519–538. Available from: [https://doi.org/10.1016/0146-6380\(88\)90144-1](https://doi.org/10.1016/0146-6380(88)90144-1)
- Christiansen, F.G. & Bojesen-Koefed, J.A. (2021) Inventory of onshore petroleum seeps and stains in Greenland: a web-based GIS model. *GEUS Bulletin*, 47, 6519. Available from: <https://doi.org/10.34194/geusb.v47.6519>
- Christiansen, F.G., Bojesen-Koefed, J.A., Dam, G., Laier, T. & Salehi, S. (2020) A review of oil and gas seepage in the Nuussuaq Basin, West

- Greenland – implications for petroleum exploration. *GEUS Bulletin*, 44, 4567. Available from: <https://doi.org/10.34194/geusb.v44.4567>
- Clark, P.U. (1994) Unstable behaviour of the Laurentide Ice Sheet over deforming sediment and its implications for climate change. *Quaternary Research*, 41(1), 19–25. Available from: <https://doi.org/10.1006/qres.1994.1002>
- Clarke, G.K.C., Collins, S.G. & Thompson, D.E. (1984) Flow, thermal structure, and subglacial conditions of a surge-type glacier. *Canadian Journal of Earth Sciences*, 21(2), 232–240. Available from: <https://doi.org/10.1139/e84-024>
- Clayton, L., Teller, J.T. & Attig, J.W. (1985) Surging of the southwestern part of the Laurentide Ice Sheet. *Boreas*, 14(3), 235–241. Available from: <https://doi.org/10.1111/j.1502-3885.1985.tb00726.x>
- Conly, F.M. (2001) Sediment sources on the lower Athabasca River, Canada: implications of natural hydrocarbon inputs from oil sand deposits. In: *Proc. 7th Fed. Interagency Sediment. Conf.*, vol. 2. Nevada, United States: United States Geological Survey, pp. 20–27.
- Czarnecki, J., Radoev, B., Schramm, L.L. & Slavchev, R. (2005) On the nature of Athabasca oil sands. *Advances in Colloid and Interface Science*, 114–115, 53–60. Available from: <https://doi.org/10.1016/j.cis.2004.09.009>
- Dalton, A.S., Margold, M., Stokes, C.R., Tarasov, L., Dyke, A.S., Adams, R.S., et al. (2020) An updated radiocarbon-based ice margin chronology for the last deglaciation of the North American ice sheet complex. *Quaternary Science Reviews*, 234, 106223. Available from: <https://doi.org/10.1016/j.quascirev.2020.106223>
- Esegbue, O., Jones, D.M., van Bergen, P.F. & Kolonic, S. (2020) Quantitative diamondoid analysis indicates oil cosourcing from a deep petroleum system onshore Niger Delta Basin. *AAPG Bulletin*, 104(6), 1231–1259. Available from: <https://doi.org/10.1306/0122201618217407>
- Evans, D.J.A. (2000) Quaternary geology and geomorphology of the Dinosaur Provincial Park area and surrounding plains, Alberta, Canada: The identification of former glacial lobes, drainage diversions and meltwater flood tracks. *Quaternary Science Reviews*, 19(10), 931–958. Available from: [https://doi.org/10.1016/S0277-3791\(99\)00029-3](https://doi.org/10.1016/S0277-3791(99)00029-3)
- Evans, D.J.A. & Campbell, I. (1992) Glacial and postglacial stratigraphy of Dinosaur Provincial Park and surrounding plains, southern Alberta, Canada. *Quaternary Science Reviews*, 11(5), 535–555. Available from: [https://doi.org/10.1016/0277-3791\(92\)90011-V](https://doi.org/10.1016/0277-3791(92)90011-V)
- Evans, D.J.A., Clark, C.D. & Rea, B.R. (2008) Landform and sediment imprints of fast glacier flow in the southwest Laurentide Ice Sheet. *Journal of Quaternary Science*, 23(3), 249–272. Available from: <https://doi.org/10.1002/jqs.1141>
- Evans, D.J.A., Phillips, E.R., Hiemstra, J.F. & Auton, C.A. (2006) Glacial till: formation, sedimentary characteristics and classification. *Earth Science Reviews*, 78(1–2), 115–176. Available from: <https://doi.org/10.1016/j.earscirev.2006.04.001>
- Evans, D.J. & Rea, B.R. (1999) Geomorphology and sedimentology of surging glaciers: a land systems approach. *Annals of Glaciology*, 28, 75–82. Available from: <https://doi.org/10.3189/172756499781821823>
- Evans, D.J.A., Young, N.J.P. & Cofaigh, C.O. (2014) Glacial geomorphology of terrestrial-terminating fast flow lobes/ice stream margins in the southwest Laurentide Ice Sheet. *Geomorphology*, 204, 86–113. Available from: <https://doi.org/10.1016/j.geomorph.2013.07.031>
- Eyles, N., Boyce, J.I. & Barendregt, R.W. (1999) Hummocky moraine: sedimentary record of stagnant Laurentide Ice Sheet lobes resting on soft beds. *Sedimentary Geology*, 123(3–4), 163–174. Available from: [https://doi.org/10.1016/S0037-0738\(98\)00129-8](https://doi.org/10.1016/S0037-0738(98)00129-8)
- Eyles, N., Eyles, C.H. & Miall, A.D. (1983) Lithofacies types and vertical profile models; an alternative approach to the description and environmental interpretation of glacial diamict and diamictite sequences. *Sedimentology*, 30(3), 393–410. Available from: <https://doi.org/10.1111/j.1365-3091.1983.tb00679.x>
- Fjeldskaar, W. & Amantov, A. (2018) Effects of glaciations on sedimentary basins. *Journal of Geodynamics*, 118, 66–81. Available from: <https://doi.org/10.1016/j.jog.2017.10.005>
- Fjeldskaar, W. & Kjemperud, A. (1992) Pleistocene glacial isostasy—implications for petroleum geology. *Norwegian Petroleum Society Special Publications*, 1(C), 187–195. Available from: <https://doi.org/10.1016/B978-0-444-88607-1.50017-6>
- Fleming, M., Fleming, I., Headley, J., Du, J. & Peru, K. (2012) Surficial bitumen in the Athabasca oil sands region, Alberta, Canada. *International Journal of Mining, Reclamation and Environment*, 26(2), 134–147. Available from: <https://doi.org/10.1080/17480930.2011.570098>
- Gibson, J.J. & Peters, D.L. (2022) Water and environmental management in oil sands regions. *Journal of Hydrology: Regional Studies*, 44, 101274. Available from: <https://doi.org/10.1016/j.ejrh.2022.101274>
- Gordon, G., Stavi, I., Shavit, U. & Rosenzweig, R. (2018) Oil spill effects on soil hydrophobicity and related properties in a hyper-arid region. *Geoderma*, 312, 114–120. Available from: <https://doi.org/10.1016/j.geoderma.2017.10.008>
- Headley, J., Akre, C., Conly, F.M., Peru, K.M. & Dickson, L. (2001) Preliminary characterization and source assessment of PAHs in tributary sediments of the Athabasca River, Canada. *Environmental Forensics*, 2(4), 335–345. Available from: <https://doi.org/10.1006/enfo.2001.0064>
- Huang, W.-Y. & Meinschein, W.G. (1979) Sterols as ecological indicators. *Geochimica et Cosmochimica Acta*, 43(5), 739–745. Available from: [https://doi.org/10.1016/0016-7037\(79\)90257-6](https://doi.org/10.1016/0016-7037(79)90257-6)
- Kishankov, A., Serov, P., Bünz, S., Patton, H., Hubbard, A., Mattingsdal, R., et al. (2022) Hydrocarbon leakage driven by Quaternary glaciations in the Barents Sea based on 2D basin and petroleum system modeling. *Marine and Petroleum Geology*, 138, 105557. Available from: <https://doi.org/10.1016/j.marpetgeo.2022.105557>
- Lee, J. (2017) Glacial lithofacies and stratigraphy. In: *Past glacial environments*, Second edition. Oxford, United Kingdom: Elsevier, pp. 377–429. Available from: <https://doi.org/10.1016/B978-0-08-100524-8.00011-7>
- Løtveit, I.F., Fjeldskaar, W. & Sydnes, M. (2019) Tilting and flexural stresses in basins due to glaciations—an example from the Barents sea. *Geosciences*, 9(11), 474. Available from: <https://doi.org/10.3390/geosciences9110474>
- Margold, M., Stokes, C.R. & Clark, C.D. (2015) Ice streams in the Laurentide Ice Sheet: Identification, characteristics and comparison to modern ice sheets. *Earth Science Reviews*, 143, 117–146. Available from: <https://doi.org/10.1016/j.earscirev.2015.01.011>
- Margold, M., Stokes, C.R. & Clark, C.D. (2018) Reconciling records of ice streaming and ice margin retreat to produce a palaeogeographic reconstruction of the deglaciation of the Laurentide Ice Sheet. *Quaternary Science Reviews*, 189, 1–30. Available from: <https://doi.org/10.1016/j.quascirev.2018.03.013>
- Margold, M., Stokes, C.R., Clark, C.D. & Kleman, J. (2015) Ice streams in the Laurentide Ice Sheet: a new mapping inventory. *Journal of Maps*, 11(3), 380–395. Available from: <https://doi.org/10.1080/17445647.2014.912036>
- McCerery, R., Esegbue, O., Jones, M., Winter, K., McHale, G. & Woodward, J. (2023) Geochemical evidence for Alberta oil sands contamination in sediments remote to known oil sands deposits in Alberta, Canada. *Environmental Forensics*. Available from: <https://doi.org/10.1080/15275922.2023.2218304>
- McCerery, R., Woodward, J., McHale, G., Winter, K., Armstrong, S., Orme, B., et al. (2021) Slippery liquid-infused porous surfaces: the effect of oil on the water repellence of hydrophobic and superhydrophobic soils. *European Journal of Soil Science*, 72(2), 963–978. Available from: <https://doi.org/10.1111/ejss.13053>
- Miall, A.D. (1977) A review of the braided-river depositional environment. *Earth Science Reviews*, 13(1), 1–62. Available from: [https://doi.org/10.1016/0012-8252\(77\)90055-1](https://doi.org/10.1016/0012-8252(77)90055-1)
- Mossop, G.D. (1980) Geology of the Athabasca oil sands. *Science*, 207(4427), 145–152. Available from: <https://doi.org/10.1126/science.207.4427.145>
- Neil, E.J. & Si, B.C. (2018) Exposure to weathering reduces the water repellency of aggregated oil sand material from subsoils of the Athabasca region. *Canadian Journal of Soil Science*, 98(2), 264–276. Available from: <https://doi.org/10.1139/cjss-2017-0087>
- Norris, S.L., Evans, D.J.A., & Cofaigh, C. Ó. (2018) Geomorphology and till architecture of terrestrial palaeo-ice streams of the southwest Laurentide Ice Sheet: a borehole stratigraphic approach. *Quaternary*

- Science Reviews, 186, 186–214. Available from: <https://doi.org/10.1016/j.quascirev.2017.12.018>
- Ó Cofaigh, C., Evans, D.J.A. & Smith, I.R. (2010) Large-scale reorganization and sedimentation of terrestrial ice streams during late Wisconsinan Laurentide Ice Sheet deglaciation. *Bulletin of the Geological Society of America*, 122(5–6), 743–756. Available from: <https://doi.org/10.1130/B26476.1>
- Paragon Soils and Environmental Consulting. (2006) Hydrocarbons in natural oil sands soils: field survey. Alberta, Canada: *Cumulative Environmental Management Association*, pp. 06–053.
- Phillips, E., Evans, D.J.A., van der Meer, J.J.M. & Lee, J.R. (2018) Microscale evidence of liquefaction and its potential triggers during soft-bed deformation within subglacial traction tills. *Quaternary Science Reviews*, 181, 123–143. Available from: <https://doi.org/10.1016/j.quascirev.2017.12.003>
- Roy, J.L. & McGill, W.B. (2000) Investigation into mechanisms leading to the development, spread and persistence of soil water repellency following contamination by crude oil. *Canadian Journal of Soil Science*, 80(4), 595–606. Available from: <https://doi.org/10.4141/S99-091>
- Roy, J.L., McGill, W.B. & Rawluk, M.D. (1999) Petroleum residues as water-repellent substances in weathered nonwettable oil-contaminated soils. *Canadian Journal of Soil Science*, 79(2), 367–380. Available from: <https://doi.org/10.4141/S97-040>
- Russell, A. (2001) Glacier surging as a control on the development of proglacial, fluvial landforms and deposits, Skeiðarársandur, Iceland. *Global and Planetary Change*, 28(1–4), 163–174. Available from: [https://doi.org/10.1016/S0921-8181\(00\)00071-0](https://doi.org/10.1016/S0921-8181(00)00071-0)
- Rutherford, R.L. (1928) Two interesting boulders in the glacial deposits of Alberta. *The Journal of Geology*, 36(6), 558–563. Available from: <https://doi.org/10.1086/623550>
- Schomacker, A., Benediktsson, Í.Ö. & Ingólfsson, Ó. (2014) The Eyjabakkajökull glacial landsystem, Iceland: geomorphic impact of multiple surges. *Geomorphology*, 218, 98–107. Available from: <https://doi.org/10.1016/j.geomorph.2013.07.005>
- Serov, P., Mattingsdal, R., Winsborrow, M., Patton, H. & Andreassen, K. (2023) Widespread natural methane and oil leakage from sub-marine Arctic reservoirs. *Nature Communications*, 14(1). <https://doi.org/10.1038/s41467-023-37514-9>
- Slomka, J.M. & Utting, D.J. (2018) Glacial advance, occupation and retreat sediments associated with multi-stage ice-dammed lakes: North-central Alberta, Canada. *Boreas*, 47(1), 150–174. Available from: <https://doi.org/10.1111/bor.12257>
- Stokes, C.R. & Clark, C.D. (2001) Palaeo-ice streams. *Quaternary Science Reviews*, 20(13), 1437–1457. Available from: [https://doi.org/10.1016/S0277-3791\(01\)00003-8](https://doi.org/10.1016/S0277-3791(01)00003-8)
- Stokes, C.R. & Clark, C.D. (2003) Laurentide ice streaming on the Canadian Shield: a conflict with the soft-bedded ice stream paradigm? *Geology*, 31(4), 347. Available from: [https://doi.org/10.1130/0091-7613\(2003\)031<0347:LISOTC>2.0.CO;2](https://doi.org/10.1130/0091-7613(2003)031<0347:LISOTC>2.0.CO;2)
- Tartan Energy Inc. (2011) Geochemical analysis to determine the origin of oil in a core sample. In: *Gushor Inc. report HDG11-001 prepared for The Hood Group*. Report submitted to Alberta Environmental Protection. Alberta, Canada: Alberta Environmental Protection.
- Tartan Energy Inc. (2012) Final investigation report for well site 15-16-057-25-W4M. In: *Report-HT1202304-01. Prepared by 950347 Alberta Ltd. o/a Hood Tech*. Report submitted to Alberta Environmental Protection. Alberta, Canada: Alberta Environmental Protection.
- Utting, D.J. & Atkinson, N. (2019) Proglacial lakes and the retreat pattern of the southwest Laurentide Ice Sheet across Alberta, Canada. *Quaternary Science Reviews*, 225, 106034. Available from: <https://doi.org/10.1016/j.quascirev.2019.106034>
- Winsborrow, M.C.M., Clark, C.D. & Stokes, C.R. (2004) Ice streams of the Laurentide Ice Sheet. *Géographie Physique et Quaternaire*, 58(2–3), 269–280. Available from: <https://doi.org/10.7202/013142ar>
- Wong, T.-S., Kang, S.H., Tang, S.K.Y., Smythe, E.J., Hatton, B.D., Grinthal, A., et al. (2011) Bioinspired self-repairing slippery surfaces with pressure-stable omniphobicity. *Nature*, 477(7365), 443–447. Available from: <https://doi.org/10.1038/nature10447>
- Woodward, J., Murray, T., Clark, R.A. & Stuart, G.W. (2003) Glacier surge mechanisms inferred from ground-penetrating radar: Kongsvegen, Svalbard. *Journal of Glaciology*, 49(167), 473–480. Available from: <https://doi.org/10.3189/172756503781830458>
- Woodward, J., Murray, T. & McCaig, A. (2002) Formation and reorientation of structure in the surge-type glacier Kongsvegen, Svalbard. *Journal of Quaternary Science*, 17(3), 201–209. Available from: <https://doi.org/10.1002/jqs.673>
- Yang, C., Wang, Z., Yang, Z., Hollebone, B., Brown, C.E., Landriault, M., et al. (2011) Chemical fingerprints of Alberta Oil Sands and related petroleum products. *Environmental Forensics*, 12(2), 173–188. Available from: <https://doi.org/10.1080/15275922.2011.574312>

SUPPORTING INFORMATION

Additional supporting information can be found online in the Supporting Information section at the end of this article.

How to cite this article: McCerery, R., Woodward, J., Winter, K., Esegbue, O., Jones, M. & McHale, G. (2023) Oil sands in glacial till as a driver of fast flow and instability in the former Laurentide Ice Sheet: Alberta, Canada. *Earth Surface Processes and Landforms*, 1–16. Available from: <https://doi.org/10.1002/esp.5700>